TECHNICAL ARTICLE

Spatial variability of elements in ancient Greek (ca. 600–250 BC) silver coins using scanning electron microscopy with energy dispersive spectrometry (SEM-EDS) and time of flight-secondary ion mass spectrometry (ToF-SIMS)

Christopher E. Marjo,[1] Gillan Davis,[2] Bin Gong,[3] and Damian B. Gore[4,a)]
[1]*Mark Wainwright Analytical Centre, University of New South Wales, NSW 2052, Australia*
[2]*Department of Ancient History, Macquarie University, NSW 2109, Australia*
[3]*Mark Wainwright Analytical Centre, University of New South Wales, Kensington, NSW 2052, Australia*
[4]*Department of Environmental Sciences, Macquarie University, NSW 2109, Australia*

(Received 11 April 2017; accepted 15 August 2017)

Archaeometrists use a variety of analytical methods to determine trace elements in ancient Greek silver coins, for provenance studies, understanding social and technological change, and authentication. One analytical problem which is little documented is understanding the horizontal spatial heterogeneity of coin elemental composition in micro-sampled areas, which are usually assumed to be uniform. This study analysed ten ancient Greek coins representative of silver circulating in the Aegean region in the sixth to third centuries BC. Scanning electron microscopy with energy dispersive spectrometry was used to map the spatial distribution of elements on coins that were abraded to remove the patina. Time of flight-secondary ion mass spectrometry was then conducted on selected coins, mapping an area ~100 × 100 μm and depth profiling from 0 to 10 μm. These data revealed the three-dimensional elemental complexity of the coins, in particular, the heterogeneity both in the patina and beneath it. These data will guide future authentication and provenance studies of larger sample sets of ancient Greek coins including the use of line scanning for laser ablation inductively coupled plasma mass spectrometry data collection rather than spot analyses, and non-destructive analytical techniques such as X-ray fluorescence spectrometry. © *2018 International Centre for Diffraction Data*. [doi:10.1017/S0885715617001002]

Key words: ancient Greek, numismatics, patina, elemental maps

I. INTRODUCTION

Numismatists and historians seek to identify the metalliferous ore bodies used to create ancient silver coins and other artefacts, and to quantify production from mining sites through the composition of coin types, as that information aids understanding of economies (especially production and trade) and political dynamics in the ancient world (Gale *et al.*, 1980; Kallithrakas-Kontos *et al.*, 2000; Giovannelli *et al.*, 2005; Sheedy and Gore, 2011; Gore and Davis, 2016; Stos-Gale and Davis, in press). Elemental analyses can also aid in authentication of coins and other artefacts, since unusual compositions may indicate that items are not genuine (e.g. Bartoli *et al.*, 2011). Lead isotope analysis is perhaps the most effective method for establishing provenance in ancient Greek coins (Stos-Gale & Gale, 2009), however, a recent study using elemental analyses from a large sample set of coins was able to successfully establish coin provenance (Gentelli, 2016). In the absence of a large number of samples, the use of lead isotopes, and other isotopes including silver and copper (e.g. Desaulty *et al.*, 2011) would be crucial to help determine provenance.

Increasingly, elemental measurements of rare and precious artefacts need to be non-destructive or at least minimally invasive. In order to achieve this, micro-sampling such as by drilling into the side of the coin and analysing the collected swarf using solution inductively coupled plasma-atomic emission spectrometry (ICP-AES) or -mass spectrometry (ICP-MS) can be undertaken (c.f. Birch *et al.*, in press). Alternatively, micro-analytical methods including laser-induced breakdown spectroscopy (LIBS), laser-ablation ICP-MS (c.f. Sarah *et al.*, 2007; Gentelli, 2016), scanning electron microscopy with energy dispersive spectrometry (SEM-EDS) or micro-X-ray fluorescence spectrometry (μ-XRF) spot analyses on very small abraded areas of coins, may be used. The size of these laser samplings or spot analyses varies according to instrument set up and researcher objectives, however regions of interest 70 μm in diameter or smaller are typical, and μ-XRF mapping may be undertaken in pixels down to 10–30 μm diameter.

A problem with micro-sampling or micro-analysis is heterogeneity of the coin composition. Although they vary from coin to coin, vertical changes in coin composition (normal to the surface) are well understood. Ancient coins may be spatially heterogeneous normal to the coin surface because of deliberate plating and pickling, environmental corrosion and development of a patina, or cleaning by collectors and curators, all of which can lead to enrichment or depletion of certain elements at the coin surfaces (e.g. Civici *et al.*, 2007; Ager *et al.*, 2013). Patina thickness varies according to coin chemistry, age, and environmental history. Patinas in ancient Greek silver coins may be as thin as 0.1 μm (Caridi *et al.*, 2012) or as

a)Author to whom correspondence should be addressed. Electronic mail: damian.gore@mq.edu.au

thick as 250 μm (Cutroneo *et al.*, 2013), reflecting the storage environment, coin preservation efforts, and cleaning.

Parallel to the coin surface, spatial heterogeneity may also occur and it is this aspect which is increasingly relevant for micro-sampling and micro-analyses. XRF mapping of a modern (1901 AD) silver coin surface revealed variations in copper and silver that were partly because of the coin surface geometry, and partly owing to compositional heterogeneity at the coin surface, and micro-polishing of the surface prior to analysis was recommended to increase analytical precision (Janssens *et al.*, 2000). Microstructural analyses of Greek silver showed intergranular fractures and cracks, infilled in places with (probable) chlorargyrite (AgCl), and inclusions up to tens of μm long, that are rich in bismuth, copper, silicon or iron (Giovannelli *et al.*, 2005). This heterogeneity can impact on the precision and accuracy of micro-sampling and micro-analysis of ancient Greek coins.

This research contributes further to the understanding of the spatial heterogeneity of a range of ancient Greek silver coins, using two methods of micro-analysis. SEM-EDS was used to map a range of common major and minor elements across the abraded surfaces of a range of coins (Table I). The more sensitive time of flight-secondary ion mass spectrometry (ToF-SIMS) was then used to map small areas and depth profiles with high sensitivity for a wide range of ions. The research is intended to optimise future studies using non-destructive or minimally-invasive analyses of more valuable coins.

II. METHODS

Ten silver coins were selected from among the Greek and Lydian minters of coins in the late Archaic and Classical periods, in order to encompass the range of elements likely to be found in the ancient Mediterranean (Table I). The coins were struck in Athens, Gela (Sicily), Miletos (ancient Ionia), Rhodes, Lydia (Western Asia Minor), Tarsos (ancient Cilicia), Thasos (near Thrace) and Abdera (Thrace) (Gore and Davis, 2016). Coins selected were heavily worn. The cleaning history of the coins is not known. Some (particularly GkAg1-3) appear to have been cleaned prior to acquisition, while others (particularly GkAg5, 9) show no evidence of past cleaning. The very low numismatic value of these ten coins enabled thorough study using destructive techniques, including preparation by abrasion which removed the patina from part of the coin, in order to expose a fresh sub-surface for imaging and analysis. All ten coins were tested using SEM-EDS, and three using ToF-SIMS.

A Hitachi TM3030 benchtop scanning electron microscope was used to collect backscattered electron images with auto-ranging power settings. Energy dispersive spectrometry was collected with four Bruker X-flash detectors with 130 eV resolution, at 15 kV, 1850 mA filament current, 100 s live time, and magnifications of ×40 and ×5000, for both surfaces as received (Supplementary Figures 1–4) and following abrasion (Supplementary Figures 5–8). Elemental data were collected from the K_α emission lines, except for Br and Ag which were collected from their L_α lines, and Au and Pb which were collected from their M_α lines.

Unabraded surfaces of three coins (GkAg4, 9, 10) (Supplementary Figure 9) were measured using a TOF. SIMS 5 instrument (ION-TOF, Münster, Germany) with a Bi cluster ion source as the analysis projectile at 30 keV and 1 pA (Bi^+) or 15 keV and 0.4 pA (Bi_3^+). The field of analysis was 100 × 100 μm for both positive and negative polarities. Sputtering in negative polarity mode was performed using a Cs^+ beam of 1 keV and 100 nA, while in positive polarity mode sputtering was performed using a O^- beam of 2 keV and 550 nA. Sputtering was performed in interlaced operation to produce a crater of 100 × 100 μm and conducted to a depth ranging from 4 to 12 μm until the majority of analyte counts stabilised. Depth profile rates were converted to nm by sputtering a polished coin under the same conditions and measuring the resulting crater depth with a KLA Tencor Alpha-Step D-600 stylus profiler, which has a vertical range of 1200 μm and sub-Angstrom depth resolution.

III. RESULTS

The abraded coin surfaces displayed heterogeneity at the ×40 and ×5000 scales examined. Elements commonly displaying heterogeneity include C, O, Al, Si, S, Cl, Cu, Br, and Pb (Figure 1; Supplementary Figures 1–4). The surfaces of the coins, while abraded are not polished, so shadowing and topography are visible, particularly in the ×5000 images. Elemental heterogeneity is visible as patches, streaks or granularity in some elements (Figure 1; Supplementary Figures 1–8).

Areal mapping using ToF-SIMS revealed spatial heterogeneity for all positive and negative ions mapped. Here, we report five relevant ions: Cr^+, Cu^+, Ag^+, Au^-, and Pb^+ (Figure 2), which are common in the coins examined. Each of these target metals shows spatial heterogeneity whether or not they are dominant (e.g. Ag^+), minor (e.g. Cu^+) or trace (e.g. Cr^+) metal (Figure 2). Spatial variability ranges from <5 μm in the case of Cr^+, to patches >75 μm long in

TABLE I. Details of the 10 test coins (after Gore and Davis 2016).

Coin ID	Denomination	Place of origin	Age (BCE)	Dimensions (mm)	Weight (g)
GkAg1	Tetradrachm	Athens (Central Greece)	449–413	25.02 × 23.07 × 5.70	17.10
GkAg2	Tetradrachm	Athens (Central Greece)	449–413	25.19 × 22.62 × 6.05	17.04
GkAg3	Tetradrachm	Athens (Central Greece)	449–413	25.32 × 22.45 × 6.20	17.01
GkAg4	Didrachm	Gela (Sicily)	490–480	18.89 × 18.87 × 3.64	8.14
GkAg5	12th Stater	Miletos (NW Turkey)	600–550	8.86 × 8.01 × 2.53	1.13
GkAg6	Drachma	Rhodes (SE Greek island)	2nd C	15.36 × 15.06 × 2.00	2.62
GkAg7	Siglos	Lydia (NW Turkey)	485	15.88 × 13.83 × 4.46	5.52
GkAg8	3/4 Obol	Tarsos (S Turkey)	4th C	10.38 × 9.55 × 1.15	0.60
GkAg9	Drachma	Abdera (NE Greece)	~365–245	14.31 × 12.55 × 1.86	2.06
GkAg10	Drachma	Thasos (N Greek island)	~520–490	15.21 × 15.75 × 2.02	3.54

https://doi.org/10.1017/S0885715617001002 Published online by Cambridge University Press

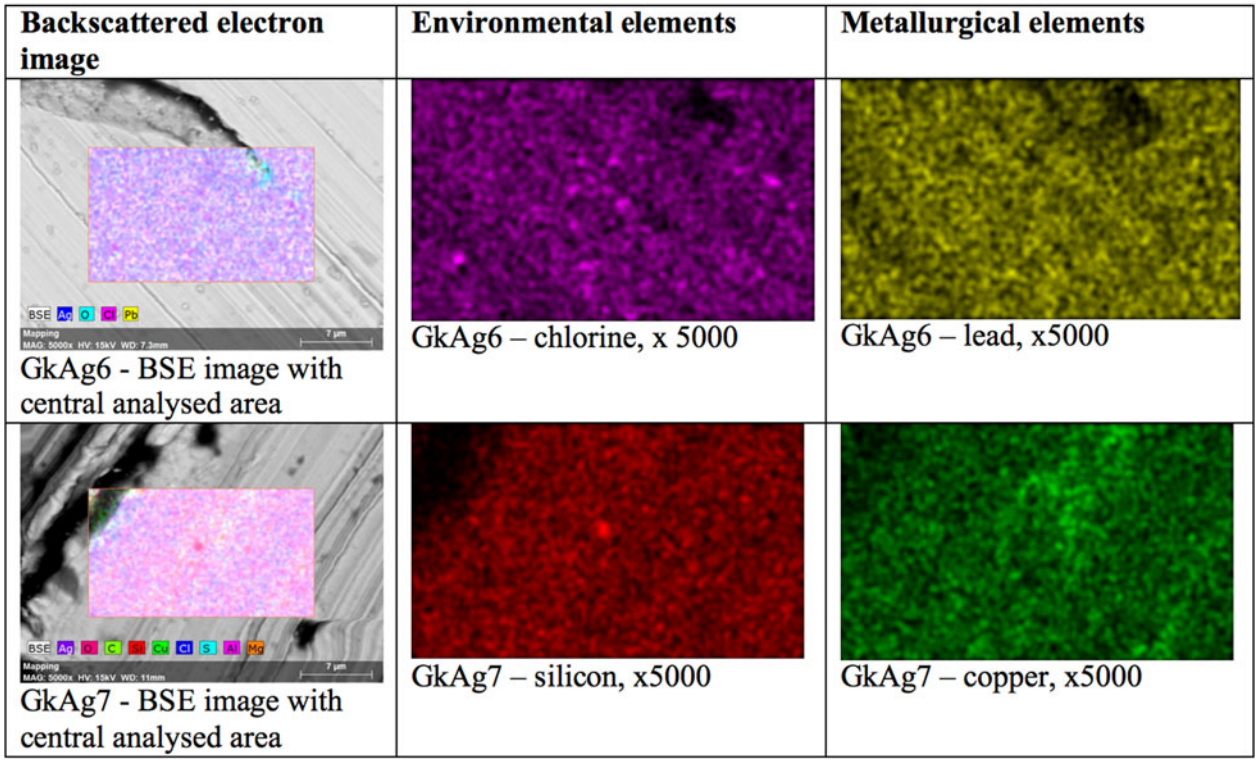

Figure 1. (Color online) Backscattered electron and X-ray elemental maps of selected elements on selected abraded coin surfaces, using SEM-EDS. The first column is a BSE image (36 × 24 μm) with the central analysed area (23 × 14 μm) highlighted; the second and third columns are ×5000 images (each 23 × 14 μm). A compendium of elemental images for each coin, for natural (unabraded) and abraded coins are in Supplementary Figures 1–4 and 5–8, respectively. Emission lines measured were Cl K_α, Si K_α, Cu K_α, and Pb M_α.

the case of Cu^+ and Pb^+. This heterogeneity is visible in both the SEM-EDS (Supplementary Figures 1–8) and TOF-SIMS (Figure 2) elemental maps.

ToF-SIMS used in depth profiling mode revealed the thickness of the patina in the abraded surfaces of the three coins. In GkAg4, elemental abundances decline from the surface to ~9 μm depth, whereas in GkAg9 and 10 they change with increasing depth until ~2 μm. In detail, the nature of the change depends on the ion being reported. Some ions change rapidly with depth with abrupt transitions, whereas others change gradually with depth. For example, GkAg4 in Figure 3 shows gradual decreases in concentration of positive ions from the surface to ~9 μm depth for B^+, Na^+, Al^+, Si^+, K^+, Ti^+, and Cr^+ and stabilise in concentration at around 9 μm depth, whereas $AgCl^+$ decreases rapidly to 2 μm and maintains that concentration thereafter. The pattern for negative ions in GkAg4 is different, with rapid changes in composition for Cl^-, Br^-, AgS^-, $AgSO_4^-$, and $AgBrCl^-$ to 0.5–1.0 μm, probably reflecting the thickness of the patina at a different part of the coin (Figure 3). The elemental profiles in GkAg9 show little change with depth, with positive ions showing generally increasing concentrations with increasing depth. Ag^+ shows a subtly lower concentration in the 3–10 μm depth, whereas B^+ and Cr^+ increase in concentration from the surface to 13 μm depth. Negative ions show a thin (<1 μm) patina and gradually decreasing concentrations with increasing depth (Figure 3). GkAg10 shows that some positive ions are concentrated in a thin (<2 μm) patina (e.g. B^+, Cr^+, Rb^+), while others exhibit fluctuations apparently unrelated to the patina thickness (e.g. Ti^+, Pb^+). Negative ions reinforce this pattern with some reflecting a thin (<1 μm) patina (e.g. Al^-, P^-, AgS^-) with others (e.g. Au^-) exhibiting patterns apparently unrelated to a patina (Figure 3).

IV. DISCUSSION

SEM-EDS elemental mapping of coin surfaces showed some elements with spatial heterogeneity (Figure 1, Supplementary Figures 5–8). While higher-performance electron microscopy was available to us, the SEM-EDS we used is relevant to researchers in the archaeometric community who can access benchtop equipment more readily. Despite this intrinsic limitation in analytical sensitivity, data from the benchtop SEM-EDS revealed important spatial heterogeneity in composition, in elements including C, O, Mg, Al, Si, S, Cl, Ca, Fe, Cu, Br, Ag, and Pb (Figure 1, Supplementary Figures 1–8). Reference to analyses on unabraded coin surfaces (Supplementary Figures 1–4) suggests that many of the heterogeneous elements are from environmental (e.g. Na, Cl, Al) rather than metallurgical (e.g. Cu, Pb) sources. There is a fine-scale granularity in the SEM-EDS elemental maps which, being visible both on the ×40 and ×5000 images (e.g. Figure 1), is probably an artefact of electronic detector noise at low concentrations during data collection. As a consequence, it is here that the much more sensitive ToF-SIMS is of particular value.

The ToF-SIMS data show that each of the main metallurgical metals studied – Cr^+, Cu^+, Ag^+, Au^+ – also exhibit granularity at a fine scale, with grains and patches of greater concentration from 3 to 5 μm diameter and larger. These grains are at spatial scales readily detected using SEM-EDS, but their concentration is presumably lower than the method

https://doi.org/10.1017/S0885715617001002 Published online by Cambridge University Press

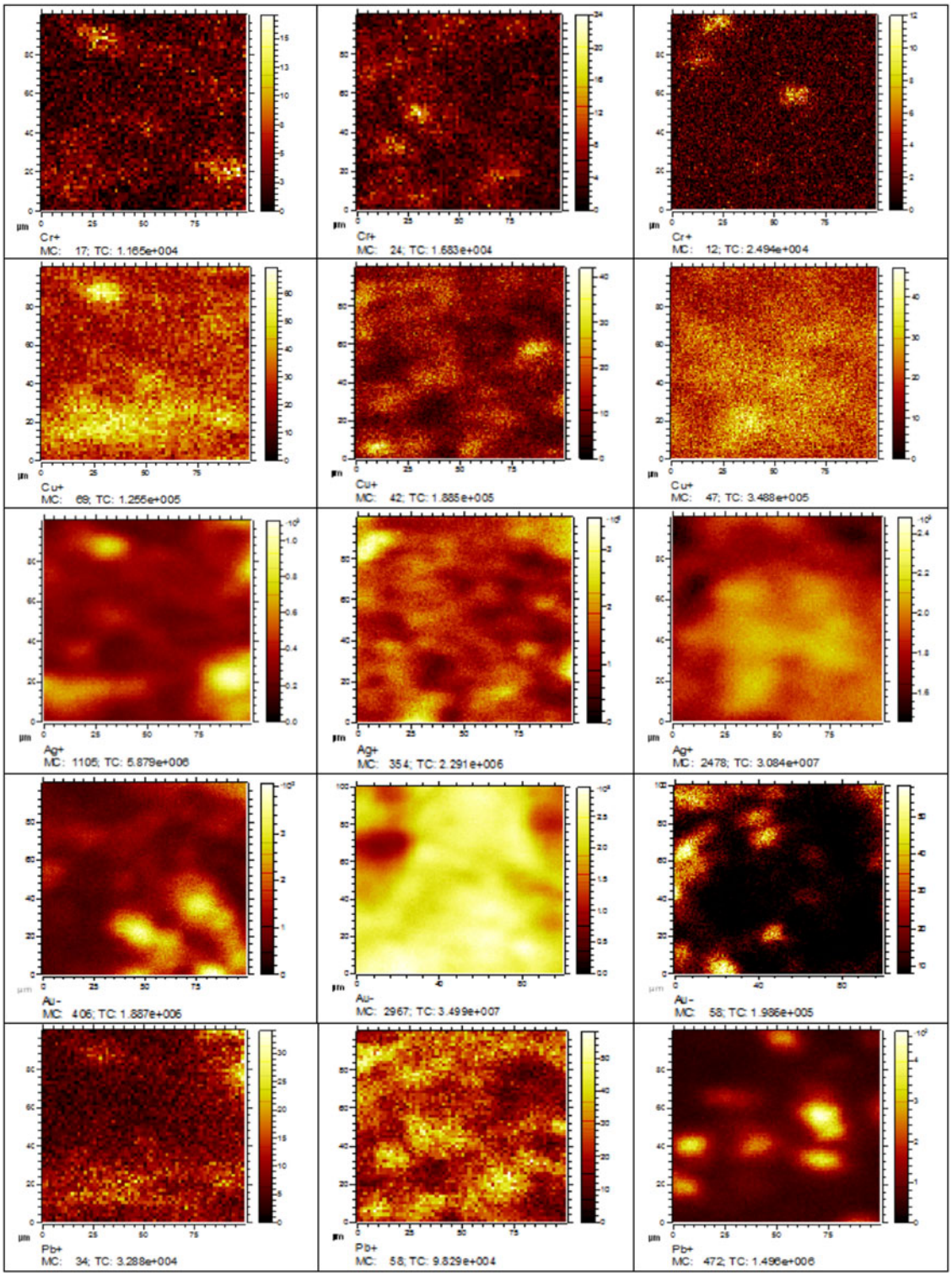

Figure 2. (Color online) Spatial maps of selected elements in three coins, using ToF-SIMS. GkAg4 is in column 1, Greek Ag9 is in column 2, and GkAg10 is in column 3. Field of view 100 × 100 μm, except for Au^- for GkAg9, 10, which is 90 × 90 μm.

detection limit of the SEM and operating conditions used, of ~0.1 wt%. Analyses conducted on the coin show the existence of the patina, but also possible grains of different composition, as seen in the depth profiles for Ti^+, Ag^+, Au^-, and Pb^+ GkAg10 (Figure 3).

Documentation of the spatial heterogeneity of ancient silver has been demonstrated for S, Cu, and Bi in metal grains, and silicon oxide and iron oxide inclusions have been documented, particularly in primary (non-remelted and re-cast) metal (Giovannelli *et al.*, 2005). Similarly, Fe, Zn, Au, Hg, and Pb have been shown to exhibit spatial variability at scales of 0.02–0.2 mm (Uzonyi *et al.*, 2000, their Fig. 3; Kantarelou *et al.*, 2011). The scale of this variability creates problems for micro-analytical methods such as LIBS and LA-ICP-MS, since the volumes sampled are small. For example, a 70 μm diameter crater would have a volume of <0.0002

https://doi.org/10.1017/S0885715617001002 Published online by Cambridge University Press

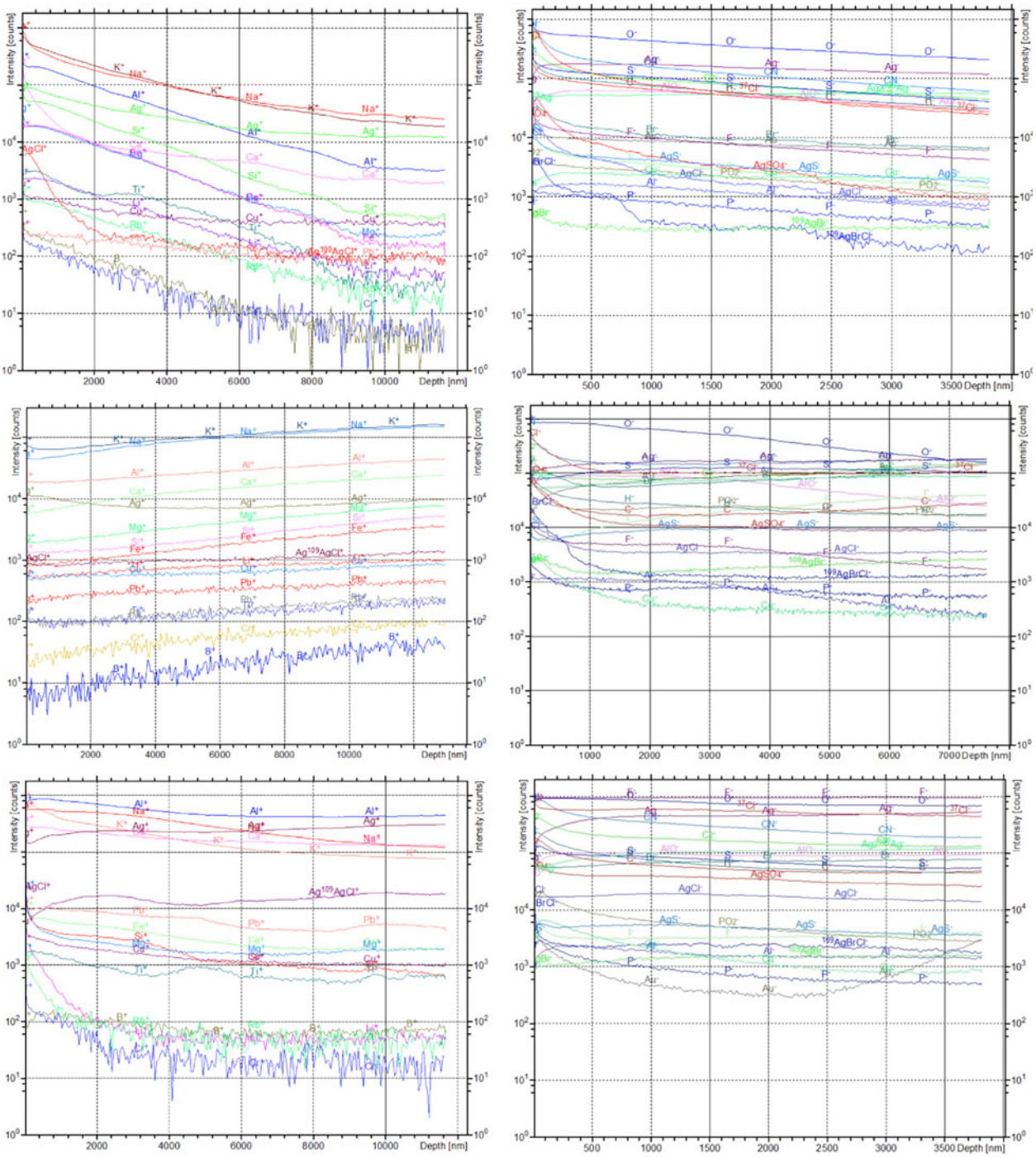

Figure 3. (Color online) Depth profiles for positive ions (left) and negative ions (right) in coins GkAg4 (row 1), GkAg9 (row 2), and GkAg10 (row 3). Measurements of positive and negative polarity ions were made on different parts of the coin.

mm^3, which might be smaller than individual metal grains with subtly different compositions.

The new data we present from the SEM-EDS (Figure 1, Supplementary Figures 1–8) and ToF-SIMS (Figures 2 and 3) mapping adds to this understanding of coin metal spatial heterogeneity. Of the ten coins we analysed in this research, three (GkAg1 - GkAg3) are of the same type and provenance and yet exhibit large relative variations in Na, Si, K, Cu, Br, Cd, Au, Pb, and Bi. Whether this variation is related to the spatial heterogeneity of the source ores or their metallurgical processing is unresolved. Either way, such inhomogeneities might be reduced with re-melting and re-casting, such as might occur through recycling of metal in the ancient world.

Microanalysis is desirable in order for "minimally invasive" analyses of rare or valuable samples, such as many ancient coins. However, the heterogeneities in coin chemistry we describe here mean that microanalytical techniques might be unrepresentative of bulk chemistry unless they are suitably replicated. Elemental images of the heterogeneities in our abraded coins suggest that analysing the swarf collected from drilling into the side of coins, might also be prone to this kind of error. In the case of LA-ICP-MS or LIBS, line

https://doi.org/10.1017/S0885715617001002 Published online by Cambridge University Press

analyses or rastering the laser across coin surfaces would help minimise analytical uncertainty, and elemental mapping might also help inform on the suitability of such microanalytical techniques on particular ancient coin surfaces.

SUPPLEMENTARY MATERIAL

The supplementary material for this article can be found at https://doi.org/10.1017/S0885715617001002

ACKNOWLEDGEMENTS

The authors thank the Australian Research Council (ARC) for financial support under project DP120103519. Part of this research was conducted at the OptoFab node of the Australian National Fabrication Facility (ANFF), using National Collaborative Research Infrastructure Strategy and New South Wales State Government funding.

Ager, F. J., Moreno-Suárez, A. I., Scrivano, S., Ortega-Feliu, I., Gómez-Tubío, B., and Respaldiza, M. A. (**2013**). "Silver surface enrichment in ancient coins studied by micro-PIXE," Nucl. Inst. Meth. Phys. Res. B **306**, 241–244.

Bartoli, L., Agresti, J., Mascalchi, M., Mencaglia, A., Cacciari, I., and Siano, S. (**2011**). "Combined elemental and microstructural analysis of genuine and fake copper-alloy coins," Quant. Electr. **41**, 663–668.

Birch, T., Kemmers, F., Klein, S., Seitz, H.-M., and Höfer, H. E. (**In press**). "Silver for the Greek colonies: issues, analysis and preliminary results from a large-scale coin sampling project," in *Metallurgy in Numismatics 6*, edited by K. Sheedy and G. Davis (Royal Numismatic Society, London).

Caridi, F., Torrisi, L., Cutroneo, M., Barreca, F., Gentile, C., Serafino, T., and Castrizio, D. (**2012**). "XPS and XRF depth patina profiles of ancient silver coins," App. Surf. Sci. **272**, 82–87.

Civici, N., Gjongecaj, Sh., Stamati, F., Dilo, T., Pavlidou, E., Polychroniadis, E. K., and Smit, Z. (**2007**). "Compositional study of IIIrd century BC silver coins from Kreshpan hoard (Albania) using EDXRF spectrometry," Nucl. Inst. Meth. Phys. Res. B **258**, 414–420.

Cutroneo, M., Torrisi, L., Caridi, F., Sayed, R., Gentile, C., Mondio, G., Serafino, T., and Castrizio, E. D. (**2013**). "Silver/oxygen depth profile in coins by using laser ablation, mass quadrupole spectrometer and X-rays fluorescence," App. Surf. Sci. **272**, 25–29.

Desaulty, A.-M., Telouk, P., Albalat, E., and Albarède, F. (**2011**). "Isotopic Ag–Cu–Pb record of silver circulation through 16th–18th century Spain," PNAS **108,** 9002–9007.

Gale, N. H., Gentner, W., and Wagner, G. A. (**1980**). "Mineralogical and geographical silver sources of archaic Greek coinage," in *Metallurgy in Numismatics 1*, edited by D. M. Metcalf and W. A. Oddy (Royal Numismatic Society, London), pp. 3–49.

Gentelli, L. (**2016**). "Provenance determination of silver artefacts from the 1629 VOC wreck Batavia using LA-ICP-MS," J.Archaeol. Sci.: Reports **9**, 536–542.

Giovannelli, G., Natali, S., Bozzini, B., Siciliano, A., Sarcinelli, G., and Vitale, R. (**2005**). "Microstructural characterization of early western Greek incuse coins," Archaeom. **47**, 817–833.

Gore, D. B. and Davis, G. (**2016**). "Suitability of transportable EDXRF for the on-site assessment of ancient silver coins and other silver artifacts," App. Spect. **70**, 840–851.

Janssens, K., Vittiglio, G., Deraedt, I., Aerts, A., Vekemans, B., Vincze, L., Wei, F., Deryck, I., Schalm, O., Adams, F., Rindby, A., Knöchel, A., Simionovici, A., and Snigirev, A. (**2000**). "Use of microscopic XRF for non-destructive analysis in art and archaeometry," X-ray Spect. **29**, 73–91.

Kallithrakas-Kontos, N., Katsanos, A. A., and Touratsoglou, J. (**2000**). "Trace element analysis of Alexander the Great's silver tetradrachms minted in Macedonia," Nucl. Inst. Meth. Phys. Res. B **171**, 342–349.

Kantarelou, V., Ager, F. J., Eugenidou, D., Chaves, F., Andreou, A., Kontou, E., Katsikosta, N., Respaldiza, M. A., Serafin, P., Sokaras, D., Zarkadas, C., Polikreti, K., and Karydas, A. G. (**2011**). "X-ray fluorescence analytical criteria to assess the fineness of ancient silver coins: application on ptolemaic coinage," Spectrochim. Acta Part B **66**, 681–690.

Sarah, G., Gratuze, B., and Barrandon, J.-N. (**2007**). "Application of laser ablation inductively coupled plasma mass spectrometry (LA-ICP-MS) for the investigation of ancient silver coins," J. Anal. Atomic Spect. **22**, 1163–1167.

Sheedy, K. and Gore, D. B. (**2011**). "Asyut 422, Seltman group P, and the imitation of attic coins," Revue Belge de Numismatique et de Sigillographie **157**, 37–54.

Stos-Gale, Z. A. and Davis, G. (**In press**). "The minting/mining nexus: new understandings of rchaic Greek silver coinage from lead isotope analysis," in *Metallurgy in Numismatics 6* edited by K. Sheedy and G. Davis (Royal Numismatic Society, London).

Stos-Gale, Z. A. and Gale, N. H. (**2009**). "Metal provenancing using isotopes and the Oxford archaeological lead isotope database (OXALID)," Archaeol. Anthropol. Sci. **1**, 195–213.

Uzonyi, I., Bugoi, R., Sasianu, A., and Kiss, Á. Z., Constantinescu, B., Torbágyi, M. (**2000**). "Characterization of Dyrrhachium silver coins by micro-PIXE method," Nucl. Inst. Meth. Phys. Res. B **161–163**, 748–752.